

Chiral Pinwheel Clusters Lacking Local Point Chirality

Kai Sun, Ting-Na Shao, Jia-Le Xie, Meng Lan, Hong-Kuan Yuan, Zu-Hong Xiong, Jun-Zhong Wang,* Ying Liu, and Qi-Kun Xue*

The supramolecular pinwheel cluster is a unique chiral structure with evident handedness. Previous studies reveal that the chiral pinwheels are composed of chiral or achiral molecules with polar groups, which result in strong intermolecular interactions such as hydrogen-bonding or dipole interactions. Herein, it is shown that the simple linear aromatic molecule, pentacene, can be self-assembled into large chiral pinwheel clusters on the semimetal Bi(111) surface, due to enhanced intermolecular interactions. The pentacene pinwheels reveal two levels of organizational chirality: the chiral hexamers resulting from asymmetric shifting along the long molecular axis, and chiral arrangement of six hexamers with a rotor motif. Furthermore, a new relation between the local point chirality and organizational chirality is identified from the pinwheels: the former is not essential for the latter in 2D pinwheel clusters of the pentacene molecule.

1. Introduction

Chirality plays an important role in physics, chemistry, and biology. Due to its potential applications in enantioselective catalysis and enantiospecific sensors, supramolecular chirality has been studied intensively in the past few years.^[1] Significant progress has been made in chiral recognition,^[2] chiral amplification,^[3] and chiral switching.^[4] Various chiral supramolecular architectures ranging from 1D chains^[5–8] and nanoscale 2D clusters^[9–13] to extended 2D domains^[14–16]

have been fabricated. Primary amongst these are the supramolecular pinwheel clusters; the unique structure with evident handedness appeared either in discrete superstructures^[9,13] or in extended 2D domains.^[17–23] It was noticed that the chiral pinwheels were formed not only by chiral molecules, but also by prochiral (2D chiral) or even achiral adsorbates, such as metal–organic complex Fe(TMA)₄ (trimesic acid, TMA),^[13] the linear NC-Ph_n-CN molecule,^[20–22] as well as the small CO molecule.^[23] Moreover, almost all the molecules within pinwheels possess polar groups, which result in strong intermolecular interactions such as hydrogen-bonding, dipole, or metal–ligand interactions. Thus, an important question here is whether achiral molecules without any polar groups can be assembled into chiral pinwheel architectures.

In principle, surface chirality can be expressed at two different levels: point chirality (local chiral motif) and organizational chirality (2D chiral domains), which represent the first and second hierarchies of 2D chirality, respectively. Recently, an intriguing result has been predicted for the chirality induced by achiral molecules: point chirality is not needed at all in 2D chiral domains of the achiral star-shaped molecules.^[24] Good registry between the molecular shape and substrate lattice leads to achiral adsorbates, which still can be organized in a chiral fashion via a close-packing interdigitation mechanism. Hence another question arises here of whether point chirality is essential to the organizational chirality in nanoscale 2D clusters.

Dr. K. Sun, T.-N. Shao, Dr. J.-L. Xie, Dr. M. Lan,
Dr. H.-K. Yuan, Prof. Z.-X. Xiong, Prof. J.-Z. Wang
School of Physical Science and Technology & MOE Key
Laboratory on Luminescence and Realtime Analysis
Southwest University
Chongqing 400715, P.R. China
E-mail: jzwangcn@swu.edu.cn

Prof. Q.-K. Xue
Department of Physics
Tsinghua University
Beijing 100084, P.R. China
E-mail: qkxue@mail.tsinghua.edu.cn

Prof. Y. Liu
Department of Physics
Hebei Normal University
Shijiazhuang 050016, P.R. China

DOI: 10.1002/smll.201200168



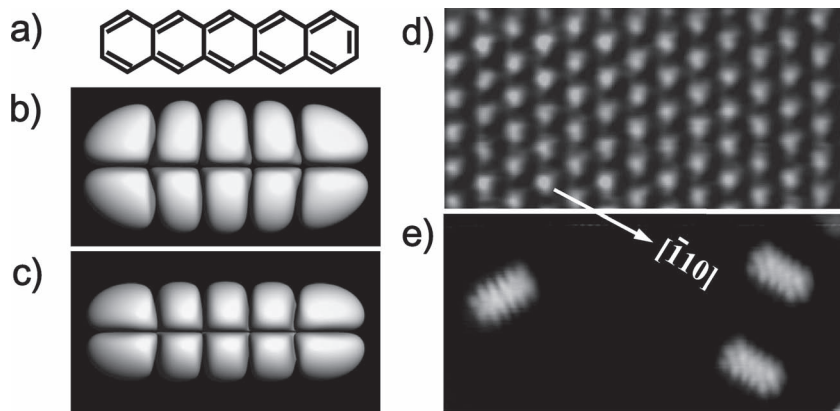


Figure 1. a) Chemical structure of the pentacene molecule. b,c) Top and side views, respectively, of the calculated HOMO for the free pentacene molecule using DFT. d) Scanning tunneling microscopy (STM) image ($56\text{ \AA} \times 28\text{ \AA}$) with atomic resolution of the Bi(111) surface. e) STM image ($130\text{ \AA} \times 65\text{ \AA}$) of isolated pentacene molecules adsorbed on the Bi(111) surface.

Pentacene ($\text{C}_{22}\text{H}_{14}$) is an achiral molecule that consists of five aromatic rings arranged in a linear fashion (Figure 1a). The semimetal Bi(111) surface has been shown to be a good template for organic epitaxial thin films.^[25] Compared with noble metal substrates, it has a much smaller density of states at the Fermi level, thus resulting in a considerably weak molecule–substrate interaction. As a result, standing-up pentacene molecules were observed even in the very first monolayer, due to the dominant intermolecular interactions.^[26] Herein, we show that, on the Bi(111) surface, pentacene molecules are self-assembled into chiral pinwheel clusters with either clockwise (R) or anticlockwise (L) handedness. Two levels of organizational chirality have been identified from the pinwheels: one is chiral hexamer formation due to asymmetric shifting along the long molecular axis; the other is the arrangement of six homochiral hexamers. Most importantly, some pentacene molecules still remain achiral within pinwheel clusters, because the molecule's and substrate's symmetry planes match precisely. Our results demonstrate that point chirality is not essential to the chiral organization in pentacene pinwheel clusters.

2. Results and Discussion

Low-temperature deposition of a small amount of pentacene onto the Bi(111) surface leads to the flat-lying orientation of isolated pentacene molecules. As shown in Figure 1e, the individual molecules exhibit pronounced features resembling the top view of electron density of the highest occupied molecular orbital (HOMO) for a free pentacene molecule (Figure 1b). The symmetric distribution of molecular protrusions implies the flat-lying orientation of pentacene molecules with the aromatic ring parallel to the substrate surface.^[27,28] Furthermore, the long molecular axes

are aligned in the high-symmetry directions of the Bi(111) substrate (Figure 1d), which indicates that the single adsorption motif of pentacene is achiral. Thus, the adsorption-induced point chirality is absent at this initial adsorption stage.

With increasing coverage, most pentacene molecules aggregate to the steps of the substrate, forming molecular nanostructures. Primary amongst these are the large pinwheel clusters possessing no mirror symmetry. Most pinwheels are composed of six curving lobes arranged in either clockwise or anticlockwise fashion, denoted as “R” or “L” handedness, respectively. The individual lobes are bent to either right or left side, denoted as “r” or “l” chirality. There is a 60° angle between every two adjacent lobes. Figure 2a presents a sample area with four R-pinwheels and

one L-pinwheel, while Figure 2b shows a sample place with two R-pinwheels and four L-pinwheels. By statistical analysis of the cluster chirality, equal numbers of R- and L-pinwheels have been observed on the substrate surface. Thus, the whole surface remains achiral at a global level, though symmetry breaking occurred at a local level. It is noticed that the pinwheel clusters exhibit either regular or irregular shapes, depending on the spacing to substrate steps. A small distance to step edges leads to irregular pinwheel formation. The pinwheels reveal a height of $\approx 3.0\text{ \AA}$, nearly twice of that (1.6 \AA) of flat-lying pentacene molecules. This implies that pentacene molecules adopt a side-lying orientation in the pinwheels. An orientational transition from flat-lying to side-lying orientation occurred in the formation process of pentacene pinwheels.

Figure 3a shows the high-resolution STM image of a regular L-pinwheel cluster. It is observed that each lobe is composed of six pentacene molecules (one hexamer) with parallel and shifted arrangement. Besides the 36 molecules within six lobes, there are eight flat-lying molecules attached to pinwheel edges. Thus, the total molecular number reaches 44 in this pinwheel. The six lobes are close-packed together

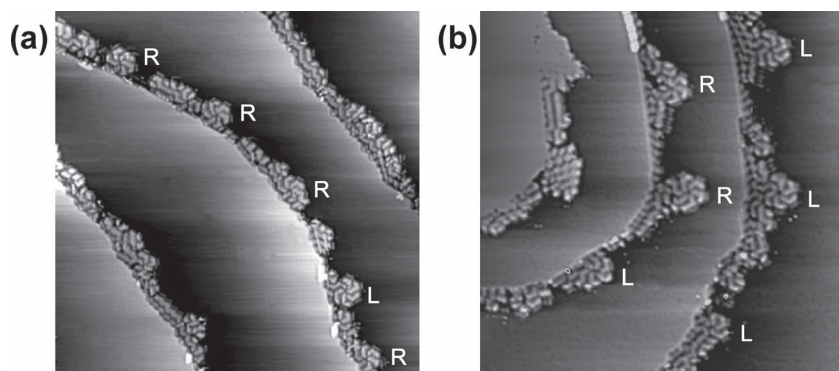


Figure 2. Pentacene pinwheel clusters formed near the steps of the Bi(111) surface. a) One sample area ($750\text{ \AA} \times 750\text{ \AA}$) containing four R-pinwheels and one L-pinwheel. b) Another sample area ($620\text{ \AA} \times 620\text{ \AA}$) containing two R-pinwheels and four L-pinwheels.

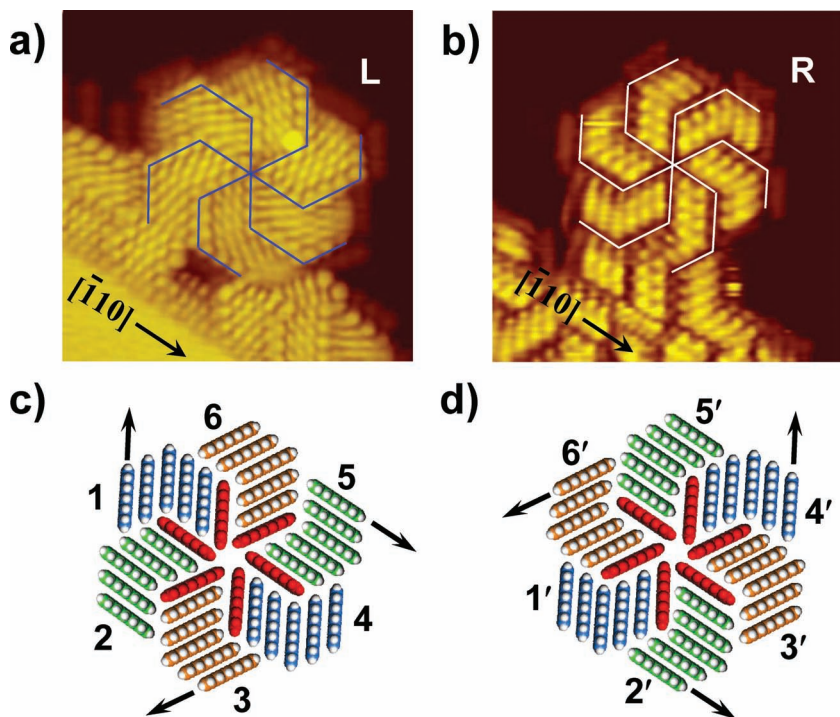


Figure 3. High-resolution STM images of regular pentacene pinwheels. a) An L-pinwheel cluster composed of 44 molecules ($88 \text{ \AA} \times 88 \text{ \AA}$, $U = -1.5 \text{ V}$). b) An R-pinwheel cluster composed of 45 pentacene molecules ($100 \text{ \AA} \times 100 \text{ \AA}$, $U = -2.5 \text{ V}$). c,d) Schematic models for the L- and R-pinwheels shown in (a) and (b), respectively. The black arrows indicate the three high-symmetry directions of the Bi(111) surface.

driven by the dominant intermolecular interactions. The six hexamers are laterally offset such that they are not pointing to the pinwheel center. As a result, organizational chirality is introduced into this pinwheel, as revealed by the red rotor motif in Figure 3c.

Each pentacene molecule manifests as five oval protrusions, resembling the side view of the HOMO of the free pentacene molecule in Figure 1c. Due to the limited lateral resolution, the nodal plane across the aromatic rings is not visible. The reflection symmetry of each oval protrusion indicates that pentacene molecules adopt a side-lying orientation (π stacking) with the aromatic rings normal to the substrate surface. Such a perpendicular orientation of the pentacene plane can be attributed to the close packing of six hexamers. Moreover, we observed that the long molecular axis is parallel to the high-symmetry directions of the Bi(111) surface. The good match between the molecule's and substrate's symmetry planes demonstrates that the individual pentacene molecules still remain achiral within this chiral pinwheel. Hence, point chirality is not a necessary condition for the organizational chirality in regular pinwheel clusters of achiral pentacene molecules. This is in agreement with the prediction of Schöck et al.^[24]

There is an asymmetric shift ($2.2 \pm 0.1 \text{ \AA}$) along the molecular long axis

between two neighboring molecules from the same hexamer. It is the asymmetric shifting that destroys the reflection symmetry of the underlying Bi(111) substrate, thereby resulting in the chirality of the hexamers. Thus, there are two levels of organizational chirality in this pinwheel: the homochiral hexamers represent the first hierarchy, while the large pinwheel cluster represents the second. More interestingly, we noticed that the asymmetric shifting is reversed to the opposite direction at the fifth molecule of a hexamer, which resulted in the curving lobes. According to force-field model calculations, the asymmetric shift in the pentacene crystal results from the interplay between van der Waals interaction and the electrostatic Coulomb interaction.^[29] From the schematic models in Figure 3c, the intermolecular interactions include the C–C interaction within π -stacked hexamers and the C–H interaction between neighboring hexamers.

It can be conceived that, if the shifting direction in an l-hexamer is reversed, the l-hexamer will change to its enantiomer, that is, the r-hexamer. If all the shifting directions in an L-pinwheel are reversed, the six l-hexamers will change to six r-hexamers, and the L-pinwheel will become an R-pinwheel. Figure 3b shows the STM image of a regular R-pinwheel cluster. The six r-hexamers constitute a pinwheel cluster with clockwise handedness. Besides the 36 side-lying molecules in the hexamers, there are nine flat-lying molecules at the periphery. Thus, the total molecular number reaches 45 in this R-pinwheel. The six r-hexamers 1'–6' shown in Figure 3d can be viewed as the enantiomers of the six l-hexamers 1–6 shown in Figure 3c. It is observed that the two terminal protrusions of a pentacene molecule become dimmed, possibly because of the intermolecular coupling between neighboring hexamers.

The STM image of an irregular L-pinwheel is displayed in **Figure 4**. There are some defects in the pinwheel interior

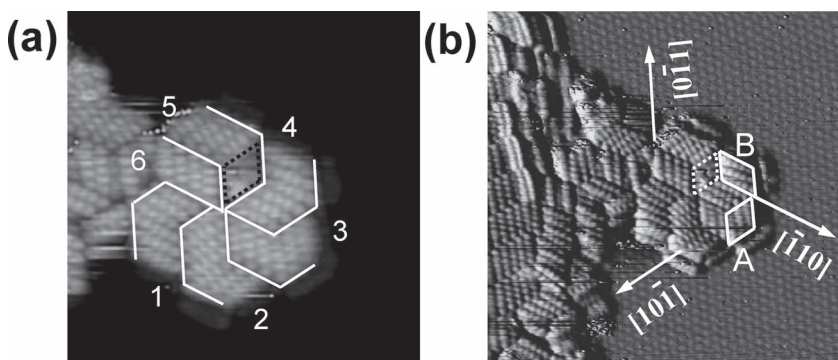


Figure 4. a) STM image of an imperfect L-pinwheel cluster ($100 \text{ \AA} \times 100 \text{ \AA}$, $U = -1.5 \text{ V}$). Dashed lines indicate the area with defects. b) STM image showing the registration of pentacene molecules with respect to the Bi(111) surface ($160 \text{ \AA} \times 160 \text{ \AA}$, $U = +2.0 \text{ V}$).

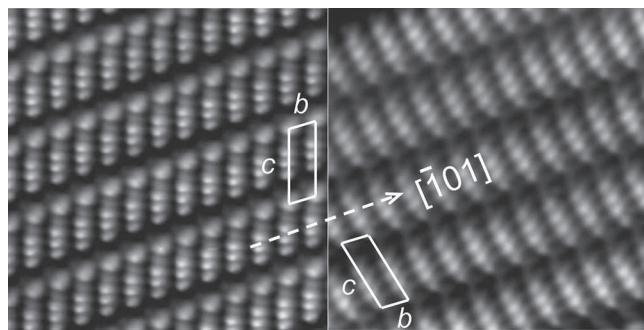


Figure 5. Enantiomorphism in 2D pentacene domains. Two mirror domains on Bi(111) together with the unit cells are displayed. Left and right panels have the same size of $72 \text{ \AA} \times 72 \text{ \AA}$ ($U = -3.5 \text{ V}$).

(marked by the dotted lines in Figure 4a). Six inequivalent lobes have been observed in this irregular pinwheel: one heptamer (lobe 2), two tetramers (lobes 5 and 6), and three hexamers (lobes 1, 3, and 4). In contrast to the regular pinwheels, the asymmetric shifting in lobe 1 occurs at the fourth molecule instead of the fifth molecule. In Figure 4b, both the individual molecules and the substrate lattice are visible simultaneously. It is observed that the six molecules within the regions A and B are not aligned with their long axis parallel to the high-symmetry directions of the Bi(111) surface, and constitute chiral adsorbates. However, most pentacene molecules remain achiral with their long axis parallel to the high-symmetry directions of the Bi(111) surface. Hence the point chirality introduced by a few pentacene molecules can be attributed to defect formation inside the cluster.

We found that pinwheel cluster formation is only restricted in the coverage far from monolayer. 2D chiral domains of pentacene molecules have been observed in the monolayer regime. There are six different chiral domains in total due to the threefold symmetry of the Bi(111) surface plus the mirror reflection element. The coexistence mirror domains suggest an overall achiral racemic surface at the global level. **Figure 5** shows two mirror domains together with their respective unit cells, where the molecular long axes are no longer aligned in the high-symmetry directions of the Bi(111) surface. The 2D pentacene domains consist of molecular rows oriented along the $[\bar{1}01]$ direction with a periodicity $b = 6.0 \text{ \AA}$ and an interrow distance $c = 16.3 \text{ \AA}$, which are very close to the lattice constants of the $b-c$ plane in pentacene crystals. The formation of pentacene crystalline domains confirms again that the intermolecular interaction is strong enough to dominate the substrate–molecule interaction.

3. Conclusion

In summary, we have demonstrated the formation of chiral pinwheel clusters of achiral pentacene molecules on the semimetal Bi(111) surface. The chiral pinwheels reveal two levels of organizational chirality: one is the chiral hexamers resulting from asymmetric shifting along the long molecular axis; the other is chiral arrangement of six hexamers with a rotor motif. The organizational chirality of pentacene pinwheels can be

rationalized by the enhanced intermolecular C–C and C–H interactions, which dominate the molecule–substrate interaction on the Bi(111) substrate. Furthermore, we demonstrated a different relation between local point chirality and organizational chirality: the former is not essential for the latter in the nanoscale 2D clusters of achiral pentacene molecules. Our results are significant for chirality construction by achiral molecules driven by enhanced intermolecular interactions.

4. Experimental Section

The experiments were conducted in a Unisoku low-temperature (LT) STM system with base pressure $\approx 1.2 \times 10^{-10} \text{ mbar}$. Bi(111) film was prepared by depositing 20 monolayers (MLs) of Bi atoms on a Si(111) 7×7 surface at room temperature with subsequent annealing at 400 K. Pentacene molecules were deposited onto a Bi(111) surface by vacuum sublimation, by heating the tantalum cell to 450 K while the sample was held at $\approx 100 \text{ K}$. The typical growth rate was about 0.02 ML min^{-1} . Constant-current STM images were acquired with the sample temperature kept at 4.3 or 78 K. After deposition of the pentacene molecules, the sample was transferred immediately to the LT STM chamber for imaging.

Supporting Information

Supporting Information is available from the Wiley Online Library or from the author.

Acknowledgements

This work was supported by the National Natural Science Foundation of China (Grant Nos. 10974156, 21173170, 91121013) and the NSF of Chongqing (CSTC, 2010BA6002).

- [1] a) S. M. Barlow, R. Raval, *Surf. Sci. Rep.* **2003**, *50*, 201–341; b) K.-H. Ernst, *Top. Curr. Chem.* **2006**, *265*, 209–252; c) R. Raval, *Chem. Soc. Rev.* **2009**, *38*, 707–721.
- [2] N. Katsonis, E. Lacaze, B. L. Feringa, *J. Mater. Chem.* **2008**, *18*, 2065–2073.
- [3] a) R. Fasel, M. Parschau, K.-H. Ernst, *Nature* **2006**, *439*, 449–452; b) S. Haq, N. Liu, V. Humblot, A. P. J. Jansen, R. Raval, *Nat. Chem.* **2009**, *1*, 409–414; c) M. Parschau, S. Romer, K.-H. Ernst, *J. Am. Chem. Soc.* **2004**, *126*, 15398–15399.
- [4] M. Parschau, D. Passerone, K.-H. Rieder, H. J. Hug, K.-H. Ernst, *Angew. Chem.* **2009**, *121*, 4125–4129; *Angew. Chem. Int. Ed.* **2009**, *48*, 4065–4068.
- [5] J. V. Barth, J. Weckesser, G. Trimarchi, M. Vladimirova, A. D. Vita, C. Cai, H. Brune, P. Gunter, K. Kern, *J. Am. Chem. Soc.* **2002**, *124*, 7991–8000.
- [6] Q. Chen, N. V. Richardson, *Nat. Mater.* **2003**, *2*, 324–328.
- [7] M. Böhringer, W. D. Schneider, R. Berndt, *Angew. Chem.* **2000**, *112*, 821–825; *Angew. Chem. Int. Ed.* **2000**, *39*, 792–795.
- [8] M. Lingenfelder, G. Tomba, G. Costantini, L. C. Ciacchi, A. D. Vita, K. Kern, *Angew. Chem.* **2007**, *119*, 4576–4579; *Angew. Chem. Int. Ed.* **2007**, *46*, 4492–4495.

- [9] M. Böhringer, K. Morgenstern, W. D. Schneider, R. Berndt, *Angew. Chem.* **1999**, *111*, 832–834; *Angew. Chem. Int. Ed.* **1999**, *38*, 821–823.
- [10] A. Kühnle, T. R. Linderoth, B. Hammer, F. Besenbacher, *Nature* **2002**, *415*, 891–893.
- [11] A. Kühnle, T. R. Linderoth, F. Besenbacher, *J. Am. Chem. Soc.* **2003**, *125*, 14680–14681.
- [12] M. C. Blüm, E. Cavar, M. Pivetta, F. Patthey, W. D. Schneider, *Angew. Chem.* **2005**, *117*, 5468–5471; *Angew. Chem. Int. Ed.* **2005**, *44*, 5334–5337.
- [13] P. Messina, A. Dmitriev, N. Lin, H. Spillmann, M. Abel, J. V. Barth, K. Kern, *J. Am. Chem. Soc.* **2002**, *124*, 14000–14001.
- [14] M. Ortega Lorenzo, C. J. Baddeley, C. Muryn, R. Raval, *Nature* **2000**, *404*, 376–379.
- [15] Y. H. Wei, K. Kannappan, G. W. Flynn, M. B. Zimmt, *J. Am. Chem. Soc.* **2004**, *126*, 5318–5322.
- [16] R. Fasel, M. Parschau, K.-H. Ernst, *Angew. Chem.* **2003**, *115*, 5336–5339; *Angew. Chem. Int. Ed.* **2003**, *42*, 5178–5181.
- [17] S. Weigelt, C. Busse, L. Petersen, E. Raals, B. Hammer, K. V. Gothelf, F. Besenbacher, T. R. Linderoth, *Nat. Mater.* **2006**, *5*, 112–117.
- [18] N. Katsonis, H. Xu, R. M. Haak, T. Kudernac, Z. Tomovic, S. George, M. van der Auweraer, A. P. J. Schenning, E. W. Meijer, B. L. Feringa, S. De Feyter, *Angew. Chem.* **2008**, *120*, 5075–5079; *Angew. Chem. Int. Ed.* **2008**, *47*, 4997–5001.
- [19] H. Spillmann, A. Dmitriev, N. Lin, P. Messina, J. V. Barth, K. Kern, *J. Am. Chem. Soc.* **2003**, *125*, 10725–10728.
- [20] F. Klappenberger, D. Kühne, W. Krenner, I. Silanes, A. Arnaud, F. J. García de Abajo, S. Klyatskaya, M. Ruben, J. V. Barth, *Nano Lett.* **2009**, *9*, 3509–3514.
- [21] U. Schlickum, R. Decker, F. Klappenberger, G. Zoppellaro, S. Klyatskaya, W. Auwärter, S. Nepli, K. Kern, H. Brune, M. Ruben, J. V. Barth, *J. Am. Chem. Soc.* **2008**, *130*, 11778–11782.
- [22] D. Kühne, F. Klappenberger, R. Decker, U. Schlickum, H. Brune, S. Klyatskaya, M. Ruben, J. V. Barth, *J. Phys. Chem. C* **2009**, *113*, 17851–17859.
- [23] H. Yoo, S. C. Fain Jr., S. Satija, L. Passell, *Phys. Rev. Lett.* **1986**, *56*, 244–247.
- [24] M. Schöck, R. Otero, S. Stojkovic, F. Hümmelink, A. Gourdon, E. Lægsgaard, I. Stensgaard, C. Joachim, F. Besenbacher, *J. Phys. Chem. B* **2006**, *110*, 12835–12838.
- [25] H. Kakuta, T. Hirahara, I. Matsuda, T. Nagao, S. Hasegawa, N. Ueno, K. Sakamoto, *Phys. Rev. Lett.* **2007**, *98*, 247601.
- [26] G. E. Thayer, J. T. Sadowski, F. M. Heringdorf, T. Sakurai, R. M. Tromp, *Phys. Rev. Lett.* **2005**, *95*, 256106.
- [27] W. H. Soe, C. Manzano, A. De Sarkar, N. Chandrasekhar, C. Joachim, *Phys. Rev. Lett.* **2009**, *102*, 176102.
- [28] J. Repp, G. Meyer, *Phys. Rev. Lett.* **2005**, *94*, 026803.
- [29] C. C. Mattheus, G. A. de Wijs, R. A. de Groot, T. T. M. Palstra, *J. Am. Chem. Soc.* **2003**, *125*, 6323–6330.

Received: January 24, 2012

Published online: April 17, 2012